Electronic Supplementary Information

Covalent Surface Modification by the Electron-Donating/Accepting π-Conjugated Chain to Effectively Tune the Electronic and Magnetic Properties of Zigzag SiC Nanoribbons

Xiaopeng Shen, Guangtao Yu*, Zengsong Zhang, Jingwei Liu, Hui Li, Xuri Huang, Wei Chen*

Laboratory of Theoretical and Computational Chemistry, Institute of Theoretical Chemistry, Jilin University, Changchun 130023, People's Republic of China

*To whom correspondence should be addressed. Email: yugt@jlu.edu.cn (G.Y.), w_chen@jlu.edu.cn (W.C.)

(I) zSiCNR-Si1-$(CH=CH)_n$-NH_2 and zSiCNR-Si3-$(CH=CH)_n$-NH_2 (n=2, 3, 4 and 6)

Table S1 The relative energies (ΔE) of different magnetic couplings to the ground state, magnetic moment of the ground state (M_{tot}), the formation energies (E_f), the electronic properties, the gap in the minority channel, and the charge of the substrate zSiCNR for the zSiCNR-Si1-$(CH=CH)_n$-NH_2 and zSiCNR-Si3-$(CH=CH)_n$-NH_2 (n=2, 3, 4 and 6) series. The NM, FM and AFM represent the nonmagnetic, ferromagnetic and antiferromagnetic spin couplings, respectively.

Systems	ΔE(meV)			M_{tot} (μ_B)	E_f (eV)	Electronic properties	The gap in minority channel(eV)	Charge of zSiCNR (|e|)
	NM	FM	AFM					
zSiCNR-Si1-$(CH=CH)_1$-NH_2	110.0	0.0*	--	1.000	-4.067	Half-metallicity	1.190	0.592
zSiCNR-Si1-$(CH=CH)_2$-NH_2	129.6	0.0*	--	1.000	-4.036	Half-metallicity	1.246	0.608
zSiCNR-Si1-$(CH=CH)_3$-NH_2	124.9	0.0*	--	1.000	-4.021	Half-metallicity	1.250	0.613
zSiCNR-Si1-$(CH=CH)_4$-NH_2	117.2	0.0*	--	1.000	-4.007	Half-metallicity	1.253	0.609
zSiCNR-Si1-$(CH=CH)_6$-NH_2	117.1	0.0*	--	1.000	-4.023	Half-metallicity	1.102	0.618
zSiCNR-Si3-$(CH=CH)_1$-NH_2	189.4	21.5	0.0	1.000	-2.078	Half-metallicity	0.344	0.566
zSiCNR-Si3-$(CH=CH)_2$-NH_2	207.5	2.4	0.0	1.000	-2.089	Half-metallicity	0.350	0.504
zSiCNR-Si3-$(CH=CH)_3$-NH_2	173.6	1.7	0.0	1.000	-2.091	Half-metallicity	0.344	0.518
zSiCNR-Si3-$(CH=CH)_4$-NH_2	173.7	2.6	0.0	1.000	-2.099	Half-metallicity	0.340	0.507
zSiCNR-Si3-$(CH=CH)_6$-NH_2	177.1	1.3	0.0	1.000	-2.100	Half-metallicity	0.331	0.470

* represents C(↑)Si(0) spin coupling, where ↑ and 0 mean the spin-up and zero local magnetic moments, respectively.

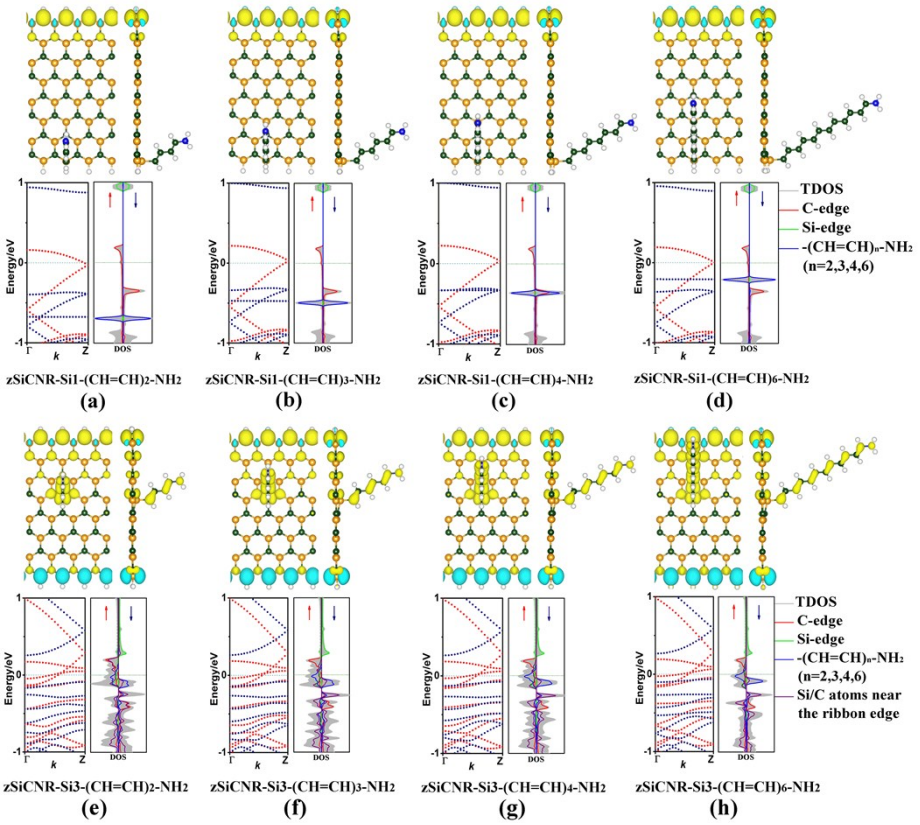

Figure S1. The geometry, band structure and corresponding DOS: (a) ~ (d) for zSiCNR-Si1-$(CH=CH)_n$-NH_2 and (e) ~ (h) for zSiCNR-Si3-$(CH=CH)_n$-NH_2 (n=2, 3, 4, 6). The yellow and blue colors in the geometrical structures represent the spin-up and spin-down orientations of the unpaired electrons, respectively. The red and blue dotted lines in the band structures denote the spin-up (↑) and spin-down (↓) channels, respectively. The Fermi-level is set as zero and indicated by the green dotted line. Note that for the substrate zSiCNR, four units are included in the used supercell.

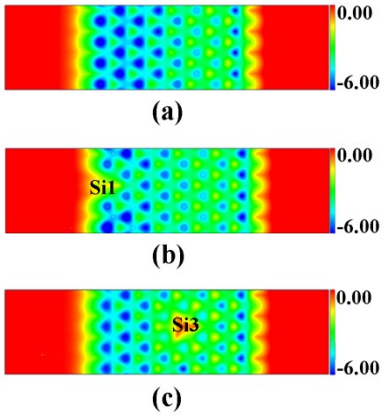

Figure S2. The distribution of electrostatic potential in the nanoribbon plane for (a) the pristine 8-zSiCNR, (b) zSiCNR-Si1-$(CH=CH)_6$-NH_2, and (c) zSiCNR-Si3-$(CH=CH)_6$-NH_2. Note that the used cross section to the plot of electrostatic potential lies near the SiC nanoribbon surface with a distance of ca. 0.2 Å between them.

(II) zSiCNR-Si1-$(CH=CH)_n$-NO_2 and zSiCNR-Si3-$(CH=CH)_n$-NO_2 (n=2, 3, 4 and 6)

Table S2 The relative energies (ΔE) of different magnetic couplings to the ground state, magnetic moment of the ground state (M_{tot}), the formation energies (E_f), the electronic properties, the gap in the minority channel, and the charge of the substrate zSiCNR for the zSiCNR-Si1-$(CH=CH)_n$-NO_2 and zSiCNR-Si3-$(CH=CH)_n$-NO_2 (n=2, 3, 4 and 6) series. The NM, FM and AFM represent the nonmagnetic, ferromagnetic and antiferromagnetic spin couplings, respectively.

Systems	ΔE(meV)			M_{tot} (μ_B)	E_f (eV)	Electronic properties	The gap in minority channel(eV)	Charge of zSiCNR (|e|)
	NM	FM	AFM					
zSiCNR-Si1-$(CH=CH)_1$-NO_2	101.6	0.0*	--	1.000	-3.966	Half-metallicity	0.693	0.695
zSiCNR-Si1-$(CH=CH)_2$-NO_2	112.3	0.0*	--	1.000	-3.912	Half-metallicity	0.620	0.704
zSiCNR-Si1-$(CH=CH)_3$-NO_2	114.5	0.0*	--	1.000	-3.940	Half-metallicity	0.605	0.672
zSiCNR-Si1-$(CH=CH)_4$-NO_2	108.8	0.0*	--	1.000	-3.954	Half-metallicity	0.590	0.663
zSiCNR-Si1-$(CH=CH)_6$-NO_2	110.3	0.0*	--	1.000	-3.943	Half-metallicity	0.556	0.656
zSiCNR-Si3-$(CH=CH)_1$-NO_2	198.1	2.3	0.0	1.000	-2.183	Half-metallicity	0.400	0.735
zSiCNR-Si3-$(CH=CH)_2$-NO_2	177.8	2.6	0.0	1.000	-2.161	Half-metallicity	0.400	0.727
zSiCNR-Si3-$(CH=CH)_3$-NO_2	200.7	14.7	0.0	1.000	-2.179	Half-metallicity	0.400	0.708
zSiCNR-Si3-$(CH=CH)_4$-NO_2	188.0	1.9	0.0	1.000	-2.170	Half-metallicity	0.384	0.704
zSiCNR-Si3-$(CH=CH)_6$-NO_2	187.0	1.0	0.0	1.000	-2.138	Half-metallicity	0.357	0.691

* represents C(↑)Si(0) spin coupling, where ↑ and 0 mean the spin-up and zero local magnetic moments, respectively.

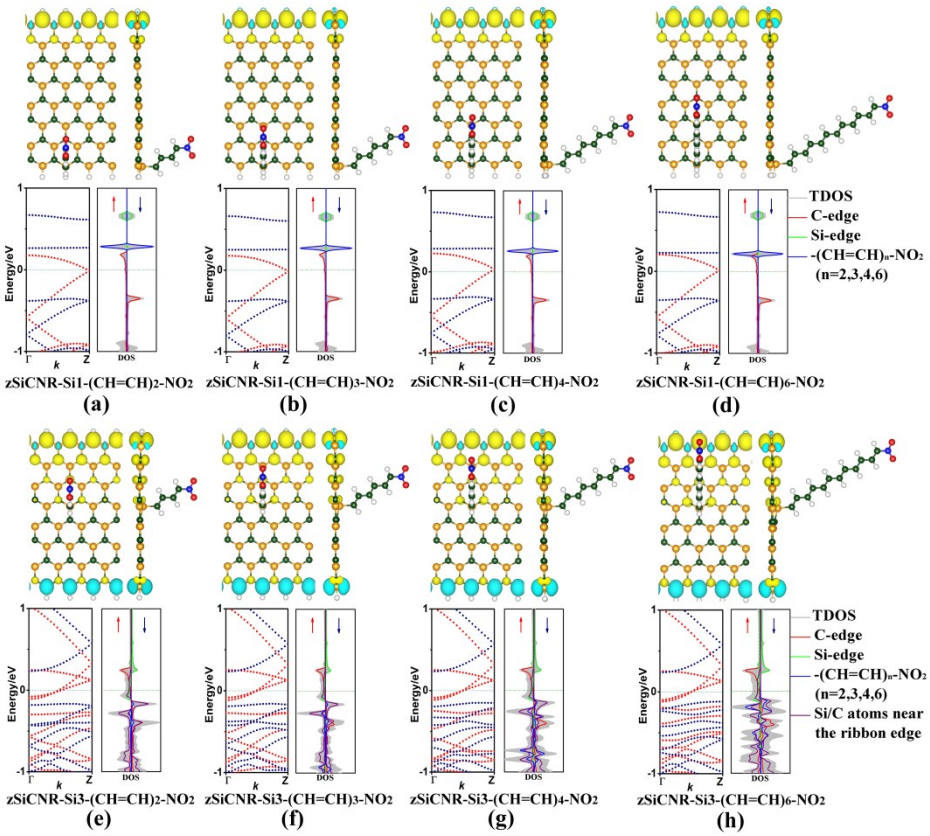

Figure S3. The geometry, band structure and corresponding DOS: (a) ~ (d) for zSiCNR-Si1-$(CH=CH)_n$-NO_2 and (e) ~ (h) for zSiCNR-Si3-$(CH=CH)_n$-NO_2 (n=2, 3, 4, 6). The yellow and blue colors in the geometrical structures represent the spin-up and spin-down orientations of the unpaired electrons, respectively. The red and blue dotted lines in the band structures denote the spin-up (↑) and spin-down (↓) channels, respectively. The Fermi-level is set as zero and indicated by the green dotted line. Note that for the substrate zSiCNR, four units are included in the used supercell.

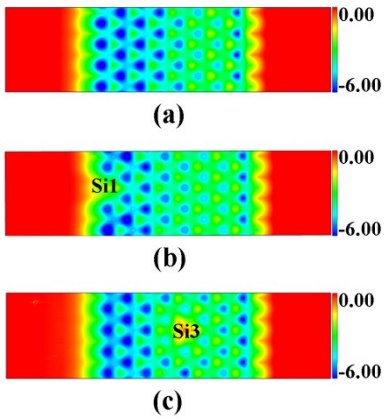

Figure S4. The distribution of electrostatic potential in the nanoribbon plane for (a) the pristine 8-zSiCNR, (b) zSiCNR-Si1-$(CH=CH)_6$-NO_2, and (c) zSiCNR-Si3-$(CH=CH)_6$-NO_2. Note that the used cross section to the plot of electrostatic potential lies near the SiC nanoribbon surface with a distance of ca. 0.2 Å between them.

（Ⅲ）The modified zSiCNR systems with the direct adsorption of NH_2 or NO_2 groups at the Si1/Si3 sites (donated by zSiCNR-Sim-NH_2 or zSiCNR-Sim-NO_2 (m=1, 3)).

Table S3 The relative energies (ΔE) of different magnetic couplings to the ground state, magnetic moment of the ground state (M_{tot}), the formation energies (E_f), the electronic property, the band gap in the minority channel of the ground state and the charge of zSiCNR for zSiCNR-Sim-NH_2, zSiCNR-Sim-NO_2 (m=1, 3). The NM, FM and AFM here represent the nonmagnetic, ferromagnetic and antiferromagnetic spin couplings, respectively.

Systems	ΔE(meV)			M_{tot} (μ_B)	E_f (eV)	Electronic properties	The gap in minority channel(eV)	Charge of zSiCNR (|e|)
	NM	FM	AFM					
zSiCNR-Si1-NH_2	105.3	0.0*	--	1.000	-4.267	Half-metallicity	1.136	0.708
zSiCNR-Si3-NH_2	182.6	1.5	0.0	1.000	-2.348	Half-metallicity	0.332	0.696
zSiCNR-Si1-NO_2	105.0	0.0*	--	1.000	-2.702	Half-metallicity	0.937	0.800
zSiCNR-Si3-NO_2	195.9	1.0	0.0	1.000	-1.051	Half-metallicity	0.400	0.848

* represent the C(↑)Si(0) spin couplings. ↑ and 0 mean the spin-up and zero local magnetic moment.

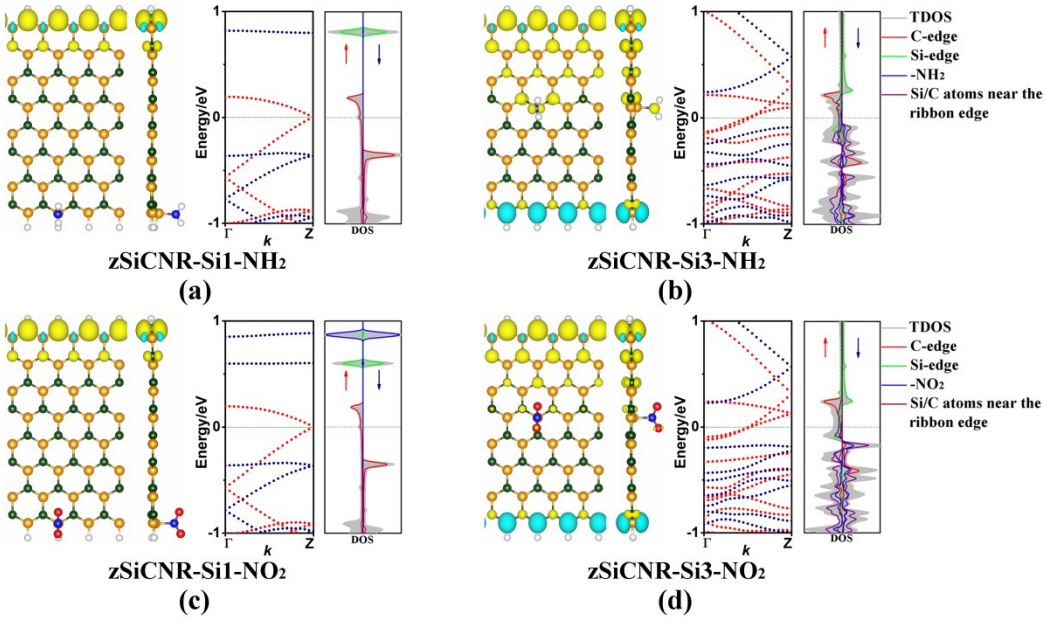

Figure S5. The geometry, spin density distribution, band structure and corresponding DOS: (a), (b) for zSiCNR-Sim-NH_2 and (c), (d) for zSiCNR-Sim-NO_2 (m=1, 3). The yellow and blue colors in the geometrical structures represent the spin-up and spin-down orientations of the unpaired electrons, respectively. The red and blue dotted lines in the band structures denote the spin-up (↑) and spin-down (↓) channels, respectively. The Fermi-level is set as zero and indicated by the green dotted line. Note that for the substrate zSiCNR, four units are included in the used supercell.

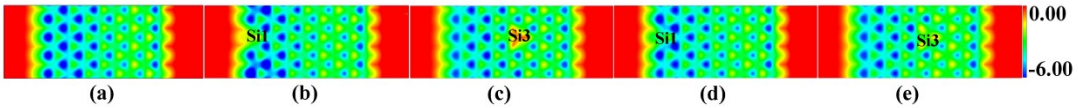

Figure S6 The distribution of electrostatic potential in the nanoribbon plane: (a) for the pristine 8-zSiCNR, (b), (c) for zSiCNR-Sim-NH_2 and (d), (e) for zSiCNR-Sim-NO_2 (m=1, 3). Note that the used cross section to the plot of electrostatic potential lies near the SiC nanoribbon surface with a distance of ca. 0.2 Å between them.

(Ⅳ) The linking of the π-conjugated -$(CH=CH)_1$-NH_2 and -$(CH=CH)_1$-NO_2

chains at the Si1 and Si3 sites of 8-zSiCNR(u) (denoted by zSiCNR(u)-Sim-$(CH=CH)_1$-NH_2 and zSiCNR(u)-Sim-$(CH=CH)_1$-NO_2 (m=1, 3; u= 5, 6), and u means that the number of the included units in the supercell for the substrate zSiCNR).

In this section, we performed the correlative computations to investigate the effect of the concentration of adsorbed π-conjugated chain on the electronic and magnetic properties of modified zSiCNR systems by linking the -$(CH=CH)_1$-NH_2 or -$(CH=CH)_1$-NO_2 chain at the representative edge Si1 and inner Si3 sites. We can understand that when increasing the number of the included unit of substrate zSiCNR in the supercell, the concentration of adsorbed π-conjugated chain is reduced for the composite systems. Here, we sampled the more five and six units included in the supercell for the substrate zSiCNR. For convenience, all these modified systems are named as zSiCNR(u)-Sim-$(CH=CH)_1$-NH_2 and zSiCNR(u)-Sim-$(CH=CH)_1$-NO_2 (m=1, 3; u= 5, 6), in which u represents the number of the included units in the supercell for the substrate zSiCNR.

Our computed results reveal that when unit number of substrate zSiCNR is increased from original four to five units, the sole FM half-metallic behaviors can be maintained in the modified zSiCNR systems by -$(CH=CH)_1$-NH_2 at the Si1 site, where the unpaired spin mainly distributes at the C edge and the unpaired spin of Si edge is still inhibited (Figure S7a). When further increasing the unit number to six for the substrate zSiCNR, the half-metallic behavior can be still sustained in the modified zSiCNR systems by -$(CH=CH)_1$-NH_2 at the Si1 site, yet the FM ground state is converted into the AFM state, where the unpaired spin of C edge is still kept and the that of Si edge is partially recovered (Figure S7e). Their computed DOS results reveal that the C edge dominates the half-metallicity in zSiCNR(5)-Si1-$(CH=CH)_1$-NH_2, while the half-metallic behavior in zSiCNR(6)-Si1-$(CH=CH)_1$-NH_2 can be determined by not only the C edge but also the Si edge of zSiCNR (Figures S7a and S7e). Comparatively, when increasing the unit number from original four to five to even six units, the sole AFM half-metallic behavior can be uniformly maintained in the modified zSiCNR systems by -$(CH=CH)_1$-NH_2 at the Si3 site. The computed DOS

results show that the edge Si atoms, the related C atoms at the side of C edge and the conjugated chain are mainly responsible for the half-metallicities in zSiCNR(5)-Si3-$(CH=CH)_1$-NH_2 and zSiCNR(6)-Si3-$(CH=CH)_1$-NH_2 (Figures S7c and S7g).

The similar situation can be also observed in the modified zSiCNR systems by $(CH=CH)_1$-NO_2 at the Si1/Si3 sites. Specifically, our computed results reveal that when increasing the unit number *u* from four to five to six, the half-metallic behavior can be kept in the zSiCNR(u)-Si1-$(CH=CH)_1$-NO_2 series, accompanied by the conversion for the FM to AFM states (Figures S7b and S7f). Additionally, the sole AFM half-metallic behavior can be also sustained in the zSiCNR(u)-Si3-$(CH=CH)_1$-NO_2 series (Figures S7d and S7h). Our computed results show that the Si edge and the related C atoms at the side of the C edge are mainly responsible for the half-metallicities for all these four systems including zSiCNR(5)-Si1-$(CH=CH)_1$-NO_2, zSiCNR(6)-Si1-$(CH=CH)_1$-NO_2, zSiCNR(5)-Si3-$(CH=CH)_1$-NO_2 and zSiCNR(6)-Si3-$(CH=CH)_1$-NO_2, as illustrated in Figure S7.

Obviously, along with the reduction of the concentration of π-conjugated chain, the magnetic degeneracy of zSiCNR can be still broken, which is also owing to the change of electrostatic potential in the ribbon plane resulted from the occurrence of the electron transfer (0.541 ~0.757 |e|) between the substrate zSiCNR and the conjugated chain (Figure S8 and Table S4). In these modified zSiCNR systems, the sole FM or AFM half-metallicity can be also achieved, where the large semiconducting gaps in minority channel with ranging from 0.367 to 0.531 eV can be observed (Table S4), indicating their considerably robust half-metallic behaviors.

Table S4 The relative energies (ΔE) of different magnetic couplings to the ground

state, magnetic moment of the ground state (M_{tot}), the formation energies (E_f), the electronic property, the band gap in the minority channel of the ground state and the charge of zSiCNR for zSiCNR(u)-Sim-$(CH{=}CH)_1$-NH_2 and zSiCNR(u)-Sim-$(CH{=}CH)_1$-NO_2 (m=1, 3; u=5, 6). The NM, FM and AFM here represent the nonmagnetic, ferromagnetic and antiferromagnetic spin couplings, respectively.

Systems	ΔE(meV)			M_{tot} (μ_B)	E_f (eV)	Electronic properties	The gap in minority channel(eV)	Charge of zSiCNR (|e|)
	NM	FM	AFM					
zSiCNR(5)-Si1-$(CH{=}CH)_1$-NH_2	92.8	0.0*	--	1.000	-4.030	Half-metallicity	0.375	0.585
zSiCNR(5)-Si3-$(CH{=}CH)_1$-NH_2	222.3	1.3	0.0	1.000	-2.112	Half-metallicity	0.367	0.541
zSiCNR(5)-Si1-$(CH{=}CH)_1$-NO_2	103.0	59.0	0.0	1.000	-3.896	Half-metallicity	0.378	0.725
zSiCNR(5)-Si3-$(CH{=}CH)_1$-NO_2	239.4	30.3	0.0	1.000	-2.271	Half-metallicity	0.465	0.717
zSiCNR(6)-Si1-$(CH{=}CH)_1$-NH_2	144.4	32.7	0.0	1.000	-4.009	Half-metallicity	0.531	0.591
zSiCNR(6)-Si3-$(CH{=}CH)_1$-NH_2	261.4	8.7	0.0	1.000	-2.171	Half-metallicity	0.384	0.556
zSiCNR(6)-Si1-$(CH{=}CH)_1$-NO_2	153.7	32.0	0.0	1.000	-3.918	Half-metallicity	0.463	0.739
zSiCNR(6)-Si3-$(CH{=}CH)_1$-NO_2	298.2	30.7	0.0	1.000	-2.301	Half-metallicity	0.496	0.757

* represent the C(↑)Si(0) spin couplings. ↑ and 0 mean the spin-up and zero local magnetic moment.

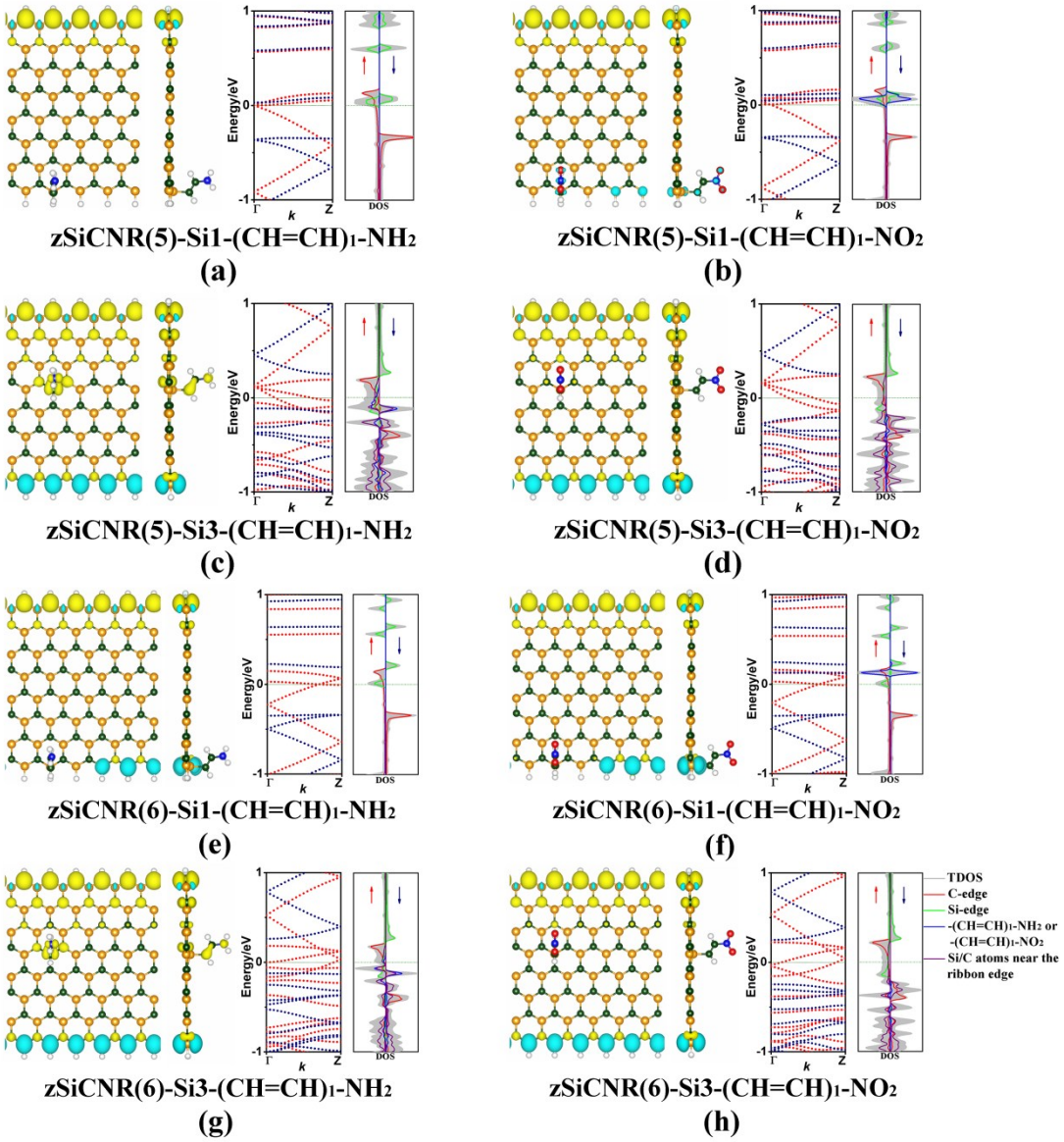

Figure S7 The geometry, spin density distribution, band structure and corresponding DOS for zSiCNR(u)-Sim-$(CH=CH)_1$-NH_2 and zSiCNR(u)-Sim-$(CH=CH)_1$-NO_2 (m=1, 3; u=5, 6). The yellow and blue colors in the geometrical structures represent the spin-up and spin-down orientations of the unpaired electrons, respectively. The red and blue dotted lines in the band structures denote the spin-up (↑) and spin-down (↓) channels, respectively. The Fermi-level is set as zero and indicated by the green dotted line.

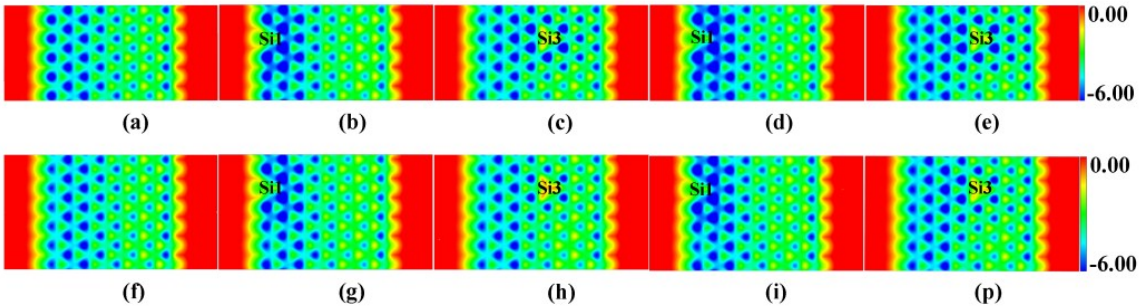

Figure S8 The distribution of electrostatic potential in the nanoribbon plane: (a) and (f) for the pristine 8-zSiCNR(u) (u=5, 6) as well as (b)~(e) and (g)~(p) for zSiCNR(u)-Sim-$(CH=CH)_1$-NH_2 and zSiCNR(u)-Sim-$(CH=CH)_1$-NO_2 (m=1, 3; u=5, 6). Note that the used cross section to the plot of electrostatic potential lies near the SiC nanoribbon surface with a distance of ca. 0.2 Å between them.